

# Model-based Control of the Magnetic Flux Profile in a Tokamak Plasma

Federico Bribiesca Argomedo<sup>1</sup>, Emmanuel Witrant<sup>1</sup>, Christophe Prieur<sup>1,2</sup>,  
Didier Georges<sup>1</sup> and Sylvain Brémond<sup>3</sup>

**Abstract**—A new model-based controller for the magnetic flux profile in a Tokamak plasma was developed using a simplified model of the magnetic flux dynamics. This simplified model is based on physically relevant dynamics that take into account the distributed nature of the system. Shape constraints on the controlled inputs are introduced, representing the limitations on the shape of the deposited current profiles by non-inductive current sources on the plasma. Some simulation results are presented and discussed.

## I. INTRODUCTION

Controlled thermonuclear fusion is based on the fusion of light nuclei such as those of tritium and deuterium at very high energies to form a heavier nucleus, such as helium. The abundance of deuterium in water and the possibility to produce tritium from lithium could make it an almost inexhaustible source of energy. Although several different nuclear fusion schemes exist (in experimental form), the Tokamak configuration is of particular interest and it has been chosen for the ongoing ITER project [12]. This project aims to demonstrate the scientific feasibility of nuclear fusion.

A detailed explanation of tokamak physics, including an overview of existing experimental facilities, can be found in [18]. An overview of current challenges in Tokamak Plasma control as well as an introduction and justification for advanced control strategies can be found in [17]. In particular, the development of suitable control schemes for sustaining what is known as advanced Tokamak operation [5, 16, 20] over long periods of time is necessary to achieve high performance in the fusion reaction. These configurations attempt to maintain a high confinement level while preserving magnetohydrodynamic (MHD) stability.

Recent advances in steady steady-state profile control can be found for instance in [7, 10, 13, 14] for JET and DIII-D. Some reviews of Tore Supra feedback control achievements can be found in [4, 8]. Yet most of these approaches are based on linear models (both discrete and distributed) identified from experimental data and are, therefore, very sensitive to operating conditions.

To address this issue, a simplified control-oriented model based on the physics of the Tokamak plasma that preserves the non-linearities of the system was developed in [19]. Using this new model, our aim is to build an adequate control

law to regulate the magnetic flux profile in steady-state operation. This is a first step toward safety-factor profile control, which has been observed to impact both the plasma energy confinement performance and the appearance of MHD instabilities. Scenarios for advanced Tokamak operation rely on non inductive current drive heating methods such as Electron Cyclotron Current Drive (ECCD), Ion Cyclotron Radio Heating (ICRH) and the Lower Hybrid Current Drive (LHCD). The latter acts both as a current source and as a heat source. The proposed results consider the LHCD operational parameters as control inputs, since we focus on the plasma current and magnetic flux control and LHCD is the most powerful steady state current drive method.

A particularity of the proposed solution is the computation of a pseudo-optimal regulator by considering the solution to an algebraic Riccati equation (ARE) in real time. The cost function used to build the dynamical version of this ARE, in the constrained version, considers the evolution of three points in the magnetic flux profile (at the center, edge and mid-radius), as well as the integral of the error at those three points. Also, shape constraints are considered for the LHCD deposition. The regulator is then tested by numerical simulation following the guidelines of [19].

This article is organized as follows: in Section II, the physical model describing the magnetic flux dynamics is presented, as well as its discretized version. In Section III, an unconstrained control law is presented and its limitations are underlined. In Section IV, a more realistic version of the control law is presented, including shape constraints on the LHCD deposition profiles. In Section V simulation results with both the unconstrained and constrained versions of the control law are presented and discussed.

## II. PROBLEM DESCRIPTION

In this article, we focus on the problem of the closed-loop regulation of the poloidal magnetic flux profile in a Tokamak plasma, defined as the flux per radian of the magnetic field  $\mathbf{B}(R, Z)$  through a disc centered on the toroidal axis at height  $Z$  and having a radius  $R$  and surface  $S$  as seen in Fig. 1.

The poloidal magnetic flux is denoted  $\psi$  and defined as:

$$\psi(R, Z) \doteq \frac{1}{2\pi} \int_S \mathbf{B}(R, Z) \cdot d\mathbf{S}$$

where  $\mathbf{B}$  is the magnetic field with poloidal component  $B_\theta$  and toroidal component  $B_\phi$ .

Using the Grad-Shafranov equilibrium equation, see [18], we can parametrize the magnetic flux  $\psi(R, Z)$  using the parameter  $\rho$  defined as  $\rho = (2\phi/B_{\phi_0})^{1/2}$ , where  $\phi(\rho, t)$  is

The authors are with: <sup>1</sup> Control Systems Department, GIPSA-lab, Grenoble, France; <sup>2</sup> LAAS-CNRS, Université of Toulouse, Toulouse, France; <sup>3</sup> Association EURATOM-CEA, CEA/IRFM, Saint Paul Lez Durance, France. E-mail: federico.bribiescaargomedo@gipsa-lab.inpg.fr

the toroidal flux per radian and  $B_{\phi_0}(t)$  is the central toroidal magnetic field, due to external coils.

Our goal is to regulate the magnetic flux profile using the non-inductive current sources, in particular the LH current drive.

### A. Magnetic Flux Dynamics

Under the assumption of negligible diamagnetic effect (caused by poloidal plasma currents) we can consider  $\rho$  to be a geometric coefficient. Also, under a large aspect ratio hypothesis ( $\rho \ll R_0$ ) we can use a cylindrical approximation of the plasma geometry. The resulting simplified diffusion equation describing the dynamics of the poloidal flux is, as stated in [19]:

$$\frac{\partial \psi}{\partial t}(\rho, t) = \frac{\eta_{\parallel}}{\mu_0} \frac{\partial^2 \psi}{\partial \rho^2} + \frac{\eta_{\parallel}}{\mu_0 \rho} \frac{\partial \psi}{\partial \rho} + \eta_{\parallel} R_0 j_{ni}$$

where  $\eta_{\parallel}(\rho, t)$  is the plasma resistivity,  $\mu_0 = 4\pi \times 10^{-7} \text{Hm}^{-1}$  is the permeability of free space,  $R_0$  is the geometric center of the plasma torus and  $j_{ni}$  is the source term due to non inductive current sources (bootstrap effect and microwave current drives).

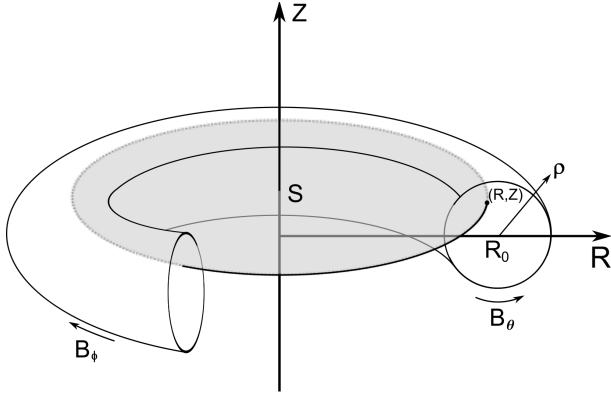


Fig. 1. Disc coordinates  $(R, Z)$  and poloidal magnetic flux surface  $S$ .

The spatial index  $\rho$  is replaced with the normalized variable  $x = \rho/a$ , where  $a$  is the minor radius corresponding to the last closed magnetic surface.  $a$  is considered constant.

The following equation is used as the reference distributed model for the system dynamics throughout this article:

$$\frac{\partial \psi}{\partial t}(x, t) = \frac{\eta_{\parallel}(x, t)}{\mu_0 a^2} \left( \frac{\partial^2 \psi}{\partial x^2} + \frac{1}{x} \frac{\partial \psi}{\partial x} \right) + \eta_{\parallel}(x, t) R_0 j_{ni} \quad (1)$$

for  $t \geq t_0$  and with initial and boundary conditions:

$$\psi(x, t_0) = a^2 B_{\phi_0} \int_x^1 \frac{r}{q(r, t_0)} dr + \psi(1, t_0) \quad , \quad \forall x \in [0, 1]$$

$$\frac{\partial \psi}{\partial x}(0, t) = 0 \quad , \quad \forall t \geq t_0 \quad (2)$$

$$\frac{\partial \psi}{\partial x}(1, t) = -\frac{R_0 \mu_0 I_p(t)}{2\pi} \quad , \quad \forall t \geq t_0 \quad (3)$$

where  $I_p(t)$  is the total plasma current and  $q(r, t_0)$  is the safety factor profile at time  $t_0$ .

The safety factor is defined as:

$$q(x, t) \doteq \frac{d\phi}{d\psi} = \frac{\partial \phi / \partial x}{\partial \psi / \partial x} \quad (4)$$

An alternative boundary condition at  $x = 1$ , instead of (3), can be chosen as:

$$\frac{\partial \psi}{\partial t}(1, t) = V_{loop}(t)$$

where  $V_{loop}$  is the flux variation at the plasma edge due to the voltage applied to the external coils. Both boundary conditions are equivalent since the voltage applied to the coils is locally regulated to maintain a desired  $I_p(t)$ .

**Remark:** In the model (1) the terms  $j_{ni}$  and  $\eta_{\parallel}$  introduce couplings (between magnetic flux diffusion, temperature and density profiles) as well as non-linearities in the diffusion equation (since  $\eta_{\parallel}$  is a function of several variables including  $\psi$ ).

**Remark:** For a more detailed description of the model used and the effect of the simplifications and assumptions made, see [19].

### B. Discretized Time-varying Dynamics

The distributed model (1) is then spatially discretized (in  $N+2$  points) using the midpoint rule to approximate the operators  $\frac{\partial^2}{\partial x^2}$  and  $\frac{1}{x} \frac{\partial}{\partial x}$ . The calculations are made to allow for a non-uniform spatial step distribution. Details of the process used for the discretization and relevant implementation details can be found in [19].

When discretizing the PDE (1) with the boundary conditions (2) and (3) and solving the finite dimensional system for the points  $x = 0$  and  $x = 1$  (using the boundary conditions), the dynamical behavior of the remaining states can be expressed as follows:

$$\dot{\psi} = A(t)\psi + B(t)j_{ni} + W(t) \quad (5)$$

where  $A(t)$  is an  $N \times N$  matrix that takes into account both the approximated differential operators and the influence of  $\eta_{\parallel}/(\mu_0 a^2)$ .  $B(t)$  is an  $N \times N$  matrix representing  $\eta_{\parallel} R_0$ .  $W(t)$  is an  $N \times 1$  column vector representing the effect of the PDE boundary conditions on the system.

### III. OPTIMAL AND PSEUDO-OPTIMAL PROFILE REGULATION WITHOUT CONSTRAINTS

Let us consider the system represented in (5). Our goal is to regulate the profile  $\psi(t)$  around a reference operating point profile  $\bar{\psi}$ . In order to have a zero steady-state error ( $\bar{\psi} - \psi$ ), an integrator is added to the system.

The extended system is then:

$$\begin{bmatrix} \dot{\psi} \\ \dot{E} \end{bmatrix} = \begin{bmatrix} A(t) & 0 \\ -\mathbb{I} & -\lambda(t) \end{bmatrix} \begin{bmatrix} \psi \\ E \end{bmatrix} + \begin{bmatrix} B(t) \\ 0 \end{bmatrix} j_{ni} + \begin{bmatrix} W(t) \\ \bar{\psi} \end{bmatrix} \quad (6)$$

where  $E$  is the integral of the error. A new parameter  $\lambda_{max} \geq \lambda(t) \geq 0$  has been introduced as a "forgetting factor" for the integrator. The purpose of this term is to avoid high overshoots when changing the operating point by weighting down past accumulated errors. It is clear that, to

avoid steady-state errors, we must have  $\lambda(t) \rightarrow 0$  as  $t \rightarrow \infty$ . This parameter is designed to vanish in finite time.

**Remark:** A bounded  $\lambda(t)$ , nonzero only when changing operating point and vanishing in finite time, allows us to preserve the overall stability of the system (provided that we change operating points only when we have already reached steady state).

Let us now detail the components of the term  $j_{ni}$  as considered in [19]:

$$j_{ni} = j_{bs} + j_{lh} + j_{ECCD}$$

where  $j_{ECCD}$  is the current due to ECCD,  $j_{lh}$  is the current deposit due to LHCD and  $j_{bs}$  is the auto-induced bootstrap current. For the purposes of this paper, we focus solely on the use of LHCD for the control of the system.

Since we have not yet introduced any input constraints, we can consider controlling the system directly with the non-inductive input  $u \doteq j_{lh} + j_{bs}$ , given that  $j_{ECCD}$  is not used. We express the extended system in the more compact form:

$$\dot{X} = A_e(t)X + B_e(t)u + W_e(t) \quad (7)$$

where

$$\begin{aligned} X &= \begin{bmatrix} \psi \\ E \end{bmatrix} \\ A_e(t) &= \begin{bmatrix} A(t) & 0 \\ -\mathbb{I} & -\lambda(t) \end{bmatrix} \\ B_e(t) &= \begin{bmatrix} B(t) \\ 0 \end{bmatrix} \\ W_e(t) &= \begin{bmatrix} W(t) \\ \bar{\psi} \end{bmatrix} \end{aligned}$$

We now consider a feedback minimizing the cost function:

$$J = \frac{1}{2} \int_{t_0}^{\infty} (X^T Q X + u^T R u) dt \quad (8)$$

with  $Q = Q^T \geq 0$  and  $R = R^T > 0$ . Classical optimality conditions for tracking control [9] lead to the following set of equations, for the optimal feedback  $u^*$ :

$$\begin{aligned} u^* &= -R^{-1}B_e^T(PX + \gamma) \\ -\dot{P} &= PA_e + A_e^T P - PB_e R^{-1}B_e^T P + Q \\ -\dot{\gamma} &= PW_e - PB_e R^{-1}B_e^T \gamma + A_e \gamma \end{aligned} \quad (9)$$

Since we are interested in implementing the resulting controller in real time, two simplifications are made in order to accelerate the online solving of the equations:

- $W(t)$  is considered almost constant, which allows us to set  $\dot{\gamma} = 0$  (this is justified since the boundary conditions depend on the operating point and since a constant value of  $I_p$  is typically desired for steady-state operation);
- $\dot{P}$  is set to zero. An algebraic Riccati equation (ARE) is thus considered (that can be solved in real time).

With these two assumptions, the resulting pseudo-optimal feedback has both feedback and feedforward terms and is:

$$\begin{aligned} u &= -R^{-1}B_e^T \left[ PX + (PB_e R^{-1}B_e^T - A_e^T)^{-1} PW_e \right] \\ 0 &= PA_e + A_e^T P - PB_e R^{-1}B_e^T P + Q \end{aligned} \quad (10)$$

**Remark:** We should stress that, since  $A_e$  and  $B_e$  are time varying, this is an approximation and, in general, not an optimal solution of the optimization problem.

**Remark:** An alternative formulation of the model could be:

$$\frac{\partial \psi}{\partial t} = \mathcal{A}(x, t)\psi + \mathcal{B}(x, t) \quad (11)$$

where  $\mathcal{A}(x, t)$  is the linear operator:

$$\mathcal{A}\psi \doteq \frac{\eta_{\parallel}}{\mu_0 a^2} \left( \frac{\partial^2 \psi}{\partial x^2} + \frac{\partial \psi}{\partial x} \right)$$

and:

$$\mathcal{B} \doteq \eta_{\parallel}(x, t)R_0$$

The dynamics of  $\psi$  as described in (11) would be a linear infinite-dimensional system on a Hilbert space. Similar results to those presented here could then be obtained, based on the analytical framework proposed in [2].

Although this feedback has been found to adequately regulate the system under simulation, the inputs are not physically realizable (the current deposition from LHCD has a particular form constraint). The shape constraints are introduced in the next section.

#### IV. PSEUDO-OPTIMAL PROFILE REGULATION UNDER SHAPE CONSTRAINTS

To include the shape constraints, an equilibrium of the original system  $(\bar{X}, \bar{u}, \bar{W}_e)$ , obtained from experimental data is considered (therefore with  $j_{lh}$  respecting the shape constraints). Defining the variables  $(\tilde{X}, \tilde{u}, \tilde{W}_e)$  as follows:

$$\begin{aligned} \tilde{X} &\doteq X - \bar{X} \\ \tilde{u} &\doteq u - \bar{u} \\ \tilde{W}_e &\doteq W_e - \bar{W}_e \end{aligned}$$

the resulting state dynamics are:

$$\dot{\tilde{X}} = A_e(t)\tilde{X} + B_e(t)\tilde{u} + \tilde{W}_e(t) \quad (12)$$

From the hypothesis that  $W_e$  is constant, used in the simplification of the feedback equations, the term  $\tilde{W}_e(t)$  can be neglected. For more details on this assumption, see the remark at the end of this section. Furthermore, around the equilibrium point, we can consider the variations in the bootstrap current as a perturbation, equating  $\tilde{u}$  directly to a variation in  $j_{lh}$ .

It has been established in [19] that the shape of LHCD deposit can be adequately approximated to a gaussian curve with parameters  $\mu$ ,  $\sigma$  and  $A_{lh}$ :

$$j_{lh} = A_{lh}(t)e^{-(x-\mu(t))^2/(2\sigma^2(t))} \quad (13)$$

Linearizing with respect to variations of the equilibrium parameters  $\bar{u}_p = (\bar{\mu}, \bar{\sigma}, \bar{A}_{lh})$ , and defining  $\tilde{u}_p$  as a variation of these parameters, the system can be rewritten as:

$$\dot{\tilde{X}} = A_e(t)\tilde{X} + B_e(t)\nabla u|_{u=\bar{u}} \tilde{u}_p$$

For simplicity in notation, we refer to  $B_e(t)\nabla u|_{u=\bar{u}}$  as  $B_p(t)$  and thus present the system as:

$$\dot{\tilde{X}} = A_e(t)\tilde{X} + B_p(t)\tilde{u}_p \quad (14)$$

The function  $u(u_p)$  being a gaussian curve, the three vectors representing the partial derivatives of  $u$  with respect to the parameters are linearly independent, which implies that the rank of  $B_p(t)$  is 3 (recall that  $B(t)$  is a diagonal matrix of rank  $N$  that accounts for  $\eta_{\parallel}R_0$ ). In turn, this guarantees that the controllability matrix of the system has at least a rank 3.

Building on the properties of the matrix  $A(t)$  we choose as a reference three points in the  $\psi$  profile:  $\psi_1$ ,  $\psi_N$  and  $\psi_{floor(N/2)}$ . It can be checked that the pair  $(A_e(t), B_p(t))$  is stabilizable for all  $t \geq t_0$ . Changing the integrator in equation (6) to evolve as  $\dot{E} = -K\psi - \lambda(t)E$ , where  $K\psi = (\psi_1, \psi_{floor(N/2)}, \psi_N)^T$ , we can choose  $Q = C^T C \geq 0$  such that the pair  $(A_e(t), C)$  is observable (in our case, weighting only the three chosen states and their integral). The fact that the pair  $(A_e(t), B_p(t))$  is stabilizable and the pair  $(A_e(t), C)$  is observable for all  $t$  ensures the existence of a positive definite solution to the ARE for all  $t \geq t_0$  (see for instance [11]).

**Remark:** Even though the pair  $(A_e(t), B_p(t))$  is stabilizable and there exists a positive definite solution to the ARE at all times the stability of the time-varying system is not guaranteed. In particular, having all closed-loop eigenvalues with negative real parts at all times is not a sufficient condition to determine the stability of such systems without an additional condition of slow-enough variation, see for instance [1, 3, 6, 15].

Using the same cost function (8) with the new value for  $Q$  and under analogous hypotheses, we can obtain a pseudo-optimal feedback for our constrained system:

$$\begin{aligned} \tilde{u}_p &= -R^{-1}B_p^T P X \\ 0 &= P A_e + A_e^T P - P B_p R^{-1} B_p^T P + Q \end{aligned} \quad (15)$$

**Remark:** Since we are neglecting the effect of  $\tilde{W}_e$  around our equilibrium, the feedforward term is no longer used, but the extension to the case where  $\tilde{W}_e$  is not negligible is trivial and should introduce a feedforward term analogous to the one presented in equation (10) without a huge computational impact. Nevertheless, tested in simulation, the improvement in the response was negligible, which seems to support the original hypotheses and therefore the proposed simplification.

## V. SIMULATION RESULTS

The proposed control laws were numerically simulated with global parameters obtained from Tore Supra shot TS-35109 ( $I_p = 0.6$  MA, power input around 1.8 MW) and a simulator built on [19]. For all the simulations, boundary conditions (2) and (3) were chosen (and not the alternate form depending on  $V_{loop}$ ). The references were chosen as well from estimations drawn from the same experimental run TS-35109, so they represent realistic values.

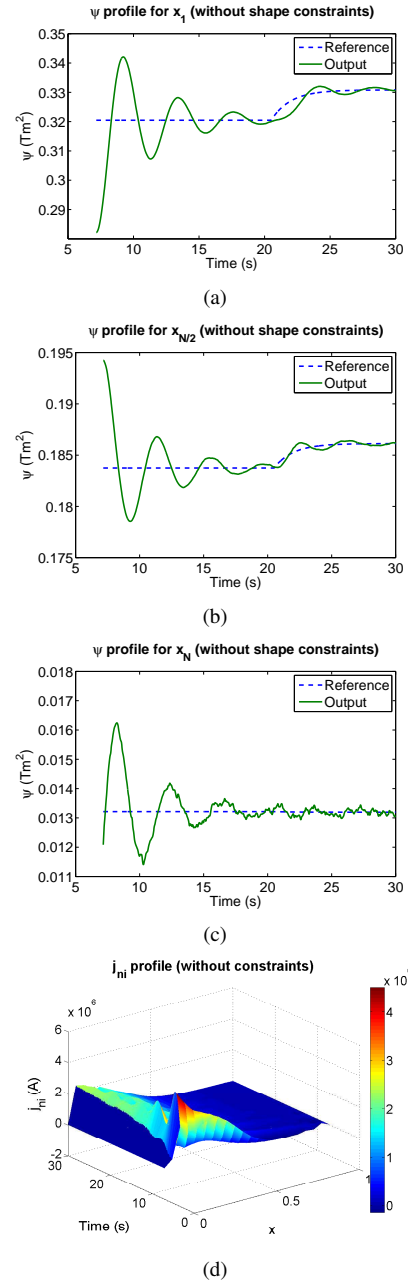


Fig. 2. Regulation around  $\bar{\psi}$  with the unconstrained controller (plain line: numerical simulation, dashed line: the reference). (a) Evolution and reference of the state  $\psi_1$ ; (b) evolution and reference of the state  $\psi_{N/2}$ ; (c) evolution and reference of the state  $\psi_N$ ; (d) applied control signal  $u$ .

### A. Controller without shape constraints

The unconstrained controller (10) was tested by numerical simulation, with its output considered directly to be  $j_{ni}$ . First, the reference was set to  $\bar{\psi}$ . At time  $t = 20$  s a reference change was applied. Fig. 2 shows the results: 2(a), (b) and (c) show the evolution of  $\psi_1$ ,  $\psi_{N/2}$  and  $\psi_N$  over time and their respective references.

It is interesting to underline that the oscillations present before the reference change are due to the fact that, when the controller is started, the "forgetting factor"  $\lambda(t)$  is set to zero and, for the unconstrained case, the regulator is

started when the system has a state far away from the desired value (since it is not the product of a linearization around some reference position). This causes a large error to accumulate and, consequently, a large overshoot followed by oscillations is seen. Nevertheless, once the reference changes (and  $\lambda$  with it) the oscillations are greatly reduced and the system reaches the desired reference with a much better performance. Tweaking the values of the weighting matrices can also improve somewhat the transient response.

Fig. 2(d) shows the values of the unconstrained input during the simulation. This input does not respect the shape constraints imposed in Section IV so it is not implementable.

### B. Controller with shape constraints

Next, the controller with shape constraints was tested by numerical simulation. This time, the system is allowed to almost reach the desired operating point by using an open-loop control (feeding the system the actual parameters from the experimental run) before activating the controller at  $t = 8$  s. This is done since the constrained version of the controller is designed to work around a particular operating point. Again, Fig. 3(a), (b), and (c) show the evolution of  $\psi_1$ ,  $\psi_{N/2}$  and  $\psi_N$  with their respective references. The results of the regulation around  $\bar{\psi}$  are quite satisfactory, even when a small change in reference is introduced (the same one used in the unconstrained simulation, also at  $t = 20$  s).

Of particular interest is the shape of  $j_{lh}$  shown in Fig. 3(d). The input to the system is always a gaussian curve, calculated from the reference parameters plus the parameter variations given by the controller. In order to compare the current profile used with both approaches (constrained and unconstrained), Fig. 3(e) shows the resulting total  $j_{ni}$  current profile when using the controller under shape constraints.

The robustness of the controller with respect to estimation errors was tested by using for the control calculations a value of  $\eta_{||}$  differing in function of  $x$  (linearly) by +10% at  $x = 0$  and -10% at  $x = 1$  from the one used to simulate the system evolution. The results can be appreciated in Fig. 4 (a), (b) and (c). In Fig. 4(a) negligible differences in the transitory behavior of the perturbed system can be appreciated, and the stabilisation time remains unchanged.

## VI. CONCLUSIONS AND PERSPECTIVES

In this paper, a new controller has been developed for the stabilization of the poloidal magnetic flux profile  $\psi$  in a Tokamak plasma, using a physically-relevant, simplified distributed model of the system dynamics. For this model, a pseudo-optimal feedback was constructed, based on the online solution of an ARE for the spatially discretized time-varying system. Furthermore, the introduction of a variable "forgetting factor"-like term in the integration of the error allows for an improvement in the transient behavior of the system. In Section III no shape constraints were considered on the current deposition of the non-inductive current sources and a global feedback-feedforward law was constructed. In Section IV a Gaussian distribution was imposed as a constraint for the  $j_{lh}$  current profile linearizing the system

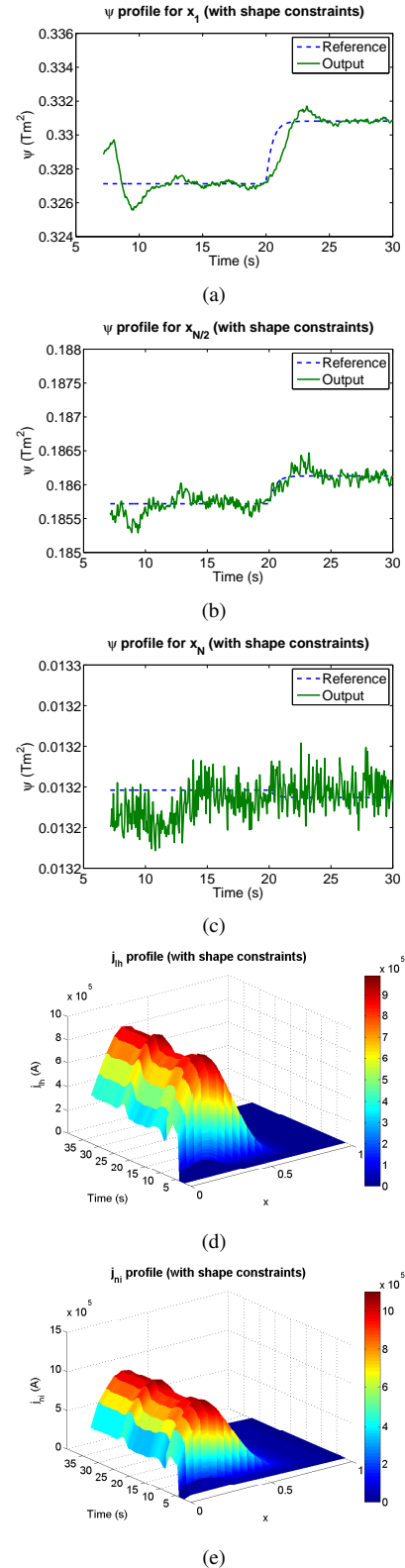


Fig. 3. Regulation around  $\bar{\psi}$  with the shape-constrained controller (plain line: numerical simulation, dashed line: the reference). (a) Evolution and reference of the state  $\psi_1$ ; (b) evolution and reference of the state  $\psi_{N/2}$ ; (c) evolution and reference of the state  $\psi_N$ ; (d) applied control signal  $u$ ; (e) resulting  $j_{ni}$ .

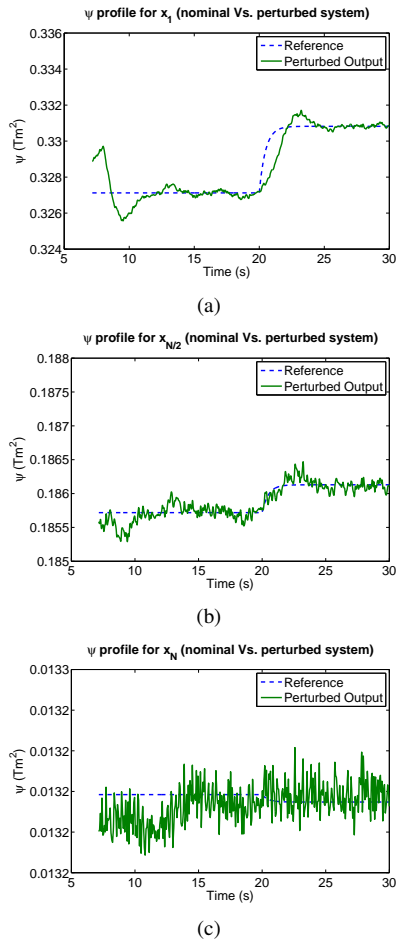


Fig. 4. Reference and perturbed output caused by an error in the estimation of  $\eta_{||}$  (dashed line: reference, solid line: numerical simulation).

dynamics around an equilibrium based on experimental data (Tore Supra shot TS-35109). It should be stressed that the time-varying nature of the system was preserved (a linear time-varying model was used as a reference). Finally, in the last section, simulation results for both the unconstrained and the constrained case are presented and discussed.

Further works will be directed to extend these results in order to provide stability guarantees for the system in general and to study its robustness. Experimental validation on Tore Supra is also expected.

## REFERENCES

- [1] F. Amato, G. Celentano, and F. Garofalo, *New sufficient conditions for the stability of slowly varying linear systems*, IEEE Transactions on Automatic Control **38** (1993), 1409–1411.
- [2] R. Curtain and H. Zwart, *An introduction to infinite-dimensional linear systems theory*, Springer Verlag, 1995.
- [3] C. A. Desoer, *Slowly varying system  $\dot{x} = a(t)x$* , IEEE Transactions on Automatic Control **14** (1969), 780–781.
- [4] G. Giruzzi et al., *Investigation of steady-state tokamak issues by long pulse experiments on Tore Supra*, Nuclear Fusion **49** (2009), no. 10, 104010.
- [5] C. Gormezano, *High performance tokamak operation regimes*, Plasma Phys. Control. Fusion **41** (1999), B367–80.
- [6] E. W. Kamen, P. P. Khargonekar, and A. Tannenbaum, *Control of slowly-varying linear systems*, IEEE Transactions on Automatic Control **34** (1989), 1283–1285.
- [7] L. Laborde, D. Mazon, D. Moreau, A. Murari, R. Felton, L. Zabeo, R. Albanese, M. Ariola, J. Bucalossi, F. Crisanti, M. de Baar, G. de Tommasi, P. de Vries, E. Joffrin, M. Lennholm, X. Litaudon, A. Pironti, T. Tala, and A. Tuccillo, *A model-based technique for integrated real-time profile control in the JET tokamak*, Plasma Phys. Control. Fusion **47** (2005), 155–183.
- [8] G. Martin, J. Bucalossi, A. Ekedahl, C. Gil, C. Grisolia, D. Guilhem, J. Gunn, F. Kazarian, D. Moulin, J. Y. Pascal, and F. Saint-Laurent, *Real time plasma feed-back control: An overview of Tore-Supra achievements*, 18th IAEA fusion energy conference, 2000.
- [9] Ján Mikleš and Miroslav Fikar, *Process modelling, identification, and control*, Springer, 2007.
- [10] D. Moreau, F. Crisanti, X. Litaudon, D. Mazon, P. de Vries, R. Felton, E. Joffrin, L. Laborde, M. Lennholm, A. Murari, V. Pericoli-Ridolfini, M. Riva, T. Tala, G. Tresset, L. Zabeo, K. D. Zastrow, and contributors to the EFDA-JET Workprogramme, *Real-time control of the q-profile in JET for steady state advanced tokamak operation*, Nucl. Fusion **43** (2003), 870–882.
- [11] M. L. Ni, *Existence condition on solutions to the algebraic riccati equation*, Acta Automatica Sinica **34** (2008), 85–87.
- [12] ITER Organization, *Official iter site: <http://www.iter.org/>*.
- [13] Y. Ou, T. C. Luce, E. Schuster, J. R. Ferron, M. L. Walker, C. Xu, and D. A. Humphreys, *Towards model-based current profile control at DIII-D*, Fusion Engineering and Design **82** (2007), 1153–1160.
- [14] Y. Ou, C. Xu, E. Schuster, T. C. Luce, J. R. Ferron, and M. L. Walker, *Extremum-seeking finite-time optimal control of plasma current profile at the DIII-D tokamak*, American Control Conference, New York, NY, 2007.
- [15] H. H. Rosenbrock, *The stability of linear time-dependent control systems*, J. Electronics and Control **15** (1963), 73–80.
- [16] T. S. Taylor, *Physics of advanced tokamaks*, Plasma Phys. Control. Fusion **39** (1997), B47–73.
- [17] M. L. Walker, E. Schuster, D. Mazon, and D. Moreau, *Open and emerging control problems in tokamak plasma control*, Proceedings of the 47th IEEE Conference on Decision and Control, Cancún, Mexico, 2008.
- [18] J. Wesson, *Tokamaks*, Third Edition, International Series of Monographs on Physics 118, Oxford University Press, 2004.
- [19] E. Witrant, E. Joffrin, S. Brémond, G. Giruzzi, D. Mazon, O. Barana, and P. Moreau, *A control-oriented model of the current control profile in tokamak plasma*, Plasma Phys. Control. Fusion **49** (2007), 1075–1105.
- [20] R. C. Wolf, *Internal transport barriers in tokamak plasmas*, Plasma Phys. Control. Fusion **45** (2003), R1–91.